Computers and Electronics in Agriculture 163 (2019) 104854

Contents lists available at ScienceDirect

Computers and Electronics in Agriculture

journal homepage: www.elsevier.com/locate/compag

Original papers

In vivo human-like robotic phenotyping of leaf traits in maize and sorghum in greenhouse

Abbas Atefi[a], Yufeng Ge[a,*], Santosh Pitla[a], James Schnable[b]

[a] Department of Biological Systems Engineering, University of Nebraska-Lincoln, Lincoln, NE 68583, USA
[b] Department of Agronomy and Horticulture, University of Nebraska-Lincoln, Lincoln, NE 68583, USA

ARTICLE INFO

Keywords:
Plant phenotyping
Leaf reflectance
Leaf temperature
Machine vision
Image processing
Agricultural robotics

ABSTRACT

In plant phenotyping, leaf-level physiological and chemical trait measurements are needed to investigate and monitor the condition of plants. The manual measurement of these properties is time consuming, error prone, and laborious. The use of robots is a new approach to accomplish such endeavors, enabling automated monitoring with minimal human intervention. In this paper, a plant phenotyping robotic system was developed to realize automated measurement of plant leaf properties. The robotic system comprised of a four Degree of Freedom (DOF) robotic manipulator and a Time-of-Flight (TOF) camera. A robotic gripper was developed to integrate an optical fiber cable (coupled to a portable spectrometer) for leaf spectral reflectance measurement, and a thermistor for leaf temperature measurement. A MATLAB program along with a Graphical User Interface (GUI) was developed to control the robotic system and its components, and for acquiring and recording data obtained from the sensors. The system was tested in a greenhouse using maize and sorghum plants. The results showed that leaf temperature measurements by the phenotyping robot were significantly correlated with those measured manually by a human researcher ($R^2 = 0.58$ for maize and 0.63 for sorghum). The leaf spectral measurements by the phenotyping robot predicted leaf chlorophyll, water content and potassium with moderate success (R^2 ranged from 0.52 to 0.61), whereas the prediction for leaf nitrogen and phosphorus were poor. The total execution time to grasp and take measurements from one leaf was 35.5 ± 4.4 s for maize and 38.5 ± 5.7 s for sorghum. Furthermore, the test showed that the grasping success rate was 78% for maize and 48% for sorghum. The phenotyping robot can be useful to complement the traditional image-based high-throughput plant phenotyping in greenhouses by collecting *in vivo* leaf-level physiological and biochemical trait measurements.

1. Introduction

With the increasing world population, agricultural production must increase to meet the demands of food, feed and fuel in the future (Rahaman et al., 2015). Climate change and lack of sufficient land to grow crops are the two major challenges that need to be addressed to produce more food (Fischer, 2009). To ensure global food security, it is necessary to monitor the interactions between plant genotype, phenotype, and environment to breed high-yielding and stress-tolerant plants (Shah et al., 2016). Plant phenotyping studies the interaction between the complex plant traits and the environment (Foix et al., 2015). It is important to perform quantitative assessment of the plant phenotypes during growing seasons (Xiao et al., 2016), which entails regular sampling and measurement of hundreds or even thousands of plants (Van Henten et al., 2006; Fourcaud et al., 2008). Traditional plant phenotyping, where data collection is largely manually, is therefore laborious and prone to error (Vijayarangan et al., 2018).

Automated monitor and measurement with agricultural robotics represents a new approach to collect plant phenotypic data (Alenyà Ribas et al., 2012). In the fields, modular phenotyping systems with various degree of automation (from manually operated carts to fully automated field robots) are developed to collect a number of diverse crop traits during growing seasons (Klose et al., 2010; Andrade-Sanchez et al., 2014; Bai et al., 2016; Shafiekhani et al., 2017; Mueller-Sim et al., 2017). More recently, gantry and cable-suspended integrated sensing and robotic systems for large-scale plant phenotype data collection were developed (Virlet et al., 2017; Kirchgessner et al., 2017; Bai et al., 2019).

Robotic systems are also developed in controlled environments (e.g., greenhouse) to realize automated phenotyping at the single plant

* Corresponding author at: Department of Biological Systems Engineering, University of Nebraska-Lincoln, Lincoln, NE 68583-0726, USA.
E-mail address: yge2@unl.edu (Y. Ge).

https://doi.org/10.1016/j.compag.2019.104854
Received 26 January 2019; Received in revised form 7 June 2019; Accepted 9 June 2019
Available online 14 June 2019
0168-1699/

level. These systems often characterize a vision system and a robotic manipulator/gripper for automated plant and leaf detection, localization, and measurement. Lu et al. (2017) mounted a TOF (Time-of-Flight) camera on the end effector of a robotic manipulator to measure the stem height and leaf length of maize seedlings, with reported errors of 13.7% and 13.1%, respectively. Chaudhury et al. (2017) attached a laser scanner to a robotic manipulator to reconstruct the 3D model of the plant and to compute its surface area and volume. A collision free robotic system was developed to probe plant leaves for indoor phenotyping (Bao et al., 2017). This system could probe all leaves of artificial plants and the average time for motion planning was 0.4 s. Ahlin et al. (2016) used an eye-in-hand camera with a six DOF (Degree of Freedom) robotic manipulator to grasp the leaves of artificial plants. The system used deep learning and visual-servoing to identify and grasp the leaves successfully.

Alenyà Ribas et al. (2012) attached a PMD CamBoard TOF camera to a robotic manipulator for probing the leaves of *Epipremnum Aureum* and *Anthurium Andreanum* plants. They also integrated a SPAD chlorophyll meter to the end effector of the robotic manipulator to measure the chlorophyll content of the leaves. The authors reported a success rate of 82% for leaf probing. Inaccurate estimation of the probing point due to poor model fitting or segmentation errors of the leaves was the main reason for this inferior performance of the robotic system.

In this paper, a robotic system was reported for *in vivo*, human-like phenotyping of leaf traits in maize and sorghum plants in the greenhouse. Two sensing modules were integrated into the robotic gripper: (1) an optical fiber cable to measure leaf VisNIR (visible and near infrared) reflectance spectra; and (2) a thermistor to measure leaf temperature. Leaf VisNIR spectra could further be used to infer an array of leaf chemical properties such as chlorophyll, water content and nitrogen content (Yendrek et al., 2017). To the best of our knowledge, such a robotic system was not previously reported. Finally, an experiment was conducted to evaluate the performance of this robotic system.

2. Materials and methods

2.1. Hardware of the robotic system

Vision system: A TOF camera (Model: SR4500, Mesa Imaging Inc., Zürich, Switzerland) was used as the vision system for the robot. This camera has a pixel array of 176 × 144 and a field of view of 69° × 55°. The accuracy of this camera is ± 2 cm in the measurement range of 0.5–5 m. The camera provides XYZ coordinates (e.g., three channels) of each pixel of the scene in camera's coordinate system. Each channel can be used to create a grayscale image of the scene.

Robotic manipulator: A four DOF robotic manipulator (Model: MICO2, KINOVA Inc., Boisbriand, Quebec, Canada) was used for this system (Fig. 1).

A robotic gripper was designed and printed using a 3D printer to integrate a bifurcated optical fiber cable (for leaf VisNIR reflectance measurement) and a thermistor (for leaf temperature measurement). The gripper was printed from black plastic material to reduce the weight and minimize light scattering (Fig. 2). The bifurcated optical fiber cable was attached to the gripper using an adjusting set screw. A small piece of neoprene rubber with low heat conductivity was attached to the gripper in order to reduce heat transfer (between the gripper and the leaves) for temperature measurement. The gripper was then attached to the end effector of the KINOVA robotic manipulator.

Sensors: The optical assembly that enabled measurement of leaf VisNIR reflectance via the bifurcated optical fiber cable (RP25, Thorlabs Inc., Newton, NJ, USA) consisted of (1) a stabilized tungsten-halogen light source (Model: SLS201, THORLABS Inc., Newton, NJ, USA) and (2) a portable spectrometer (Model: Flame, OceanOptics Inc., Dunedin, FL, USA). The output of the light source had a spectral range from 300 to 2600 nm, and the spectral range of the portable spectrometer was 350–1000 nm. The thermistor for leaf temperature measurement (Model: ST 200: Fine-Wire Thermistor, Apogee Instruments Inc., Logan, UT, USA) had a measurement accuracy of 0.2 °C between 0 and 70 °C and a response time of less than 1 s.

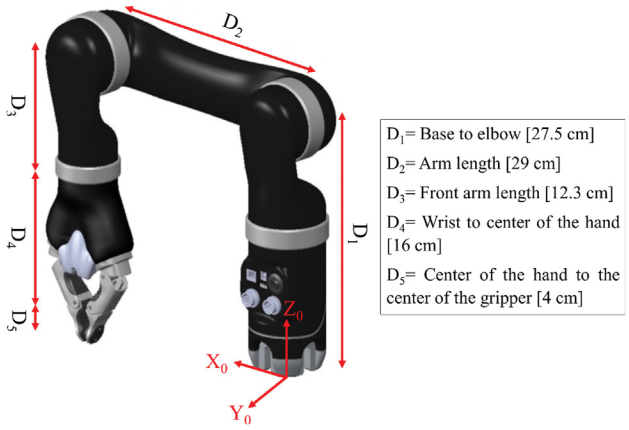

Fig. 1. The four degree of freedom robotic manipulator used in this study and its kinematic parameters.

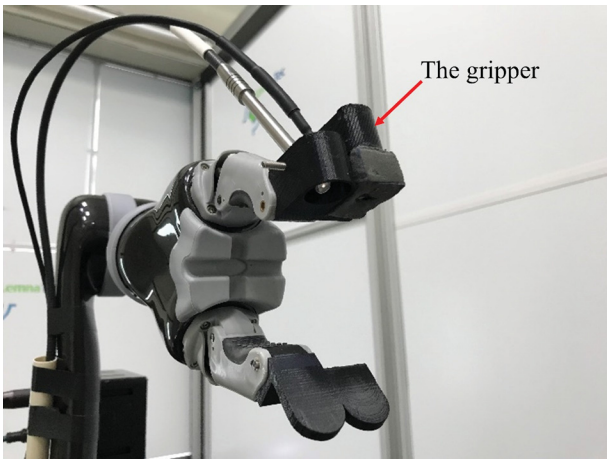

Fig. 2. The gripper and its integration onto the robotic manipulator.

A data logger (Model: LabJack U6, LabJack Corporation, Lakewood, CO, USA) was used to record data from the temperature sensor. A laptop with Intel Core i7 Processor (2.5 GHz) and 8 GB RAM was used to control the robotic system, and measure and store the data.

Integration of hardware for the phenotyping robotic system: The robotic system was mounted on the top of a height adjustable desk. This allowed the robotic system to adjust its height according to the height of plants if needed. The TOF camera was placed near to the robotic manipulator. The bifurcated optical fiber and the temperature sensor were integrated with the robotic manipulator by attaching them to the gripper (Fig. 3). Other system components including the portable spectrometer, the light source, and the data logger were also placed on the desk (Fig. 3).

2.2. Software of the robotic system

Image processing for plant segmentation, leaf identification, and grasping point localization: After taking the image using the TOF camera, the Z channel of the scene (plant) was extracted as a grayscale image (Fig. 4a). A threshold based on the distance between the camera and the plant in Z direction was determined to segment the plant from the background, and to create a binary image (Fig. 4b).

The even columns of pixels were removed from the binary image. The remaining odd columns appeared as vertical lines in the image as shown in Fig. 4c. All vertical lines were labeled. For each vertical line,

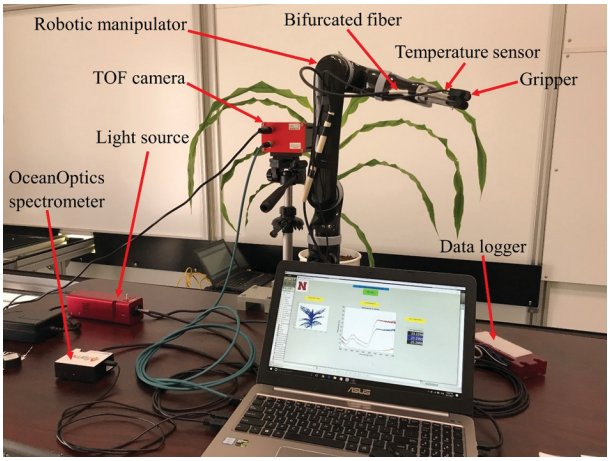

Fig. 3. The robotic system and its components.

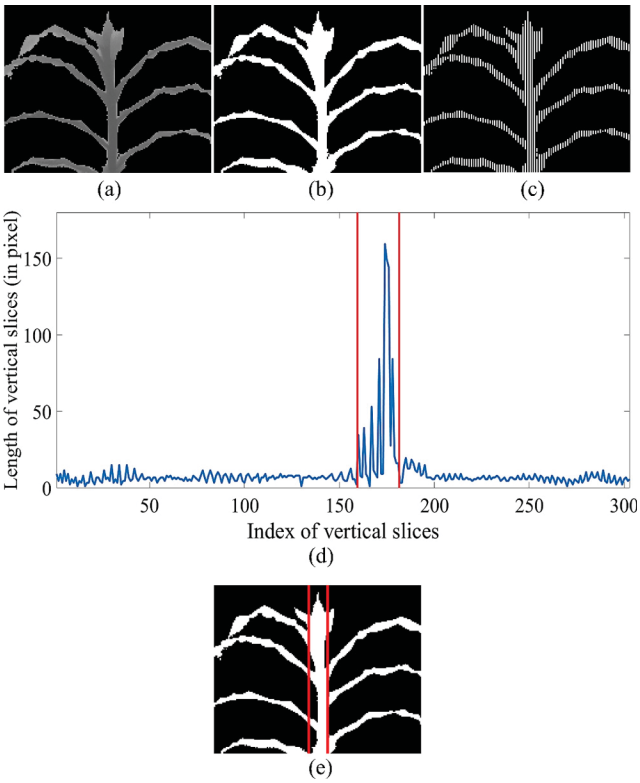

Fig. 4. (a) Grayscale image of the plant, (b) Binary image after segmentation, (c) Binary image after removing the even columns of pixels, (d) Major axis length versus the index of the vertical lines, and (e) Detected edges of the stem.

the coordinates of its center point and its length were determined. Then the length of each line was plotted against its label (Fig. 4d). Since the edges of the stem had the largest length and caused abrupt changes in the plot, the two abrupt changes and their indices were determined. The indices were used to find the center point of the edges of the stem. The stem was detected using the coordinates of the edges (Fig. 4e).

The center point of a leaf was chosen to avoid hitting the stem by the robotic manipulator, and also to grasp the leaf properly. After detecting the stem in the image, the stem was removed and the remaining leaves were labeled. The center point of each leaf along with its 3D coordinates in the camera coordinate system was determined in the binary image as a potential grasping point. A flowchart describing the process of finding the grasping point of the leaves is presented in Fig. 5.

The leaves were ranked to select the best three leaves for measurement (Fig. 6). Two criteria were considered to rank the leaves. Firstly, a leaf having a larger major axis length was given higher rank because it had greater chance to be grasped by the gripper. Secondly, a leaf which had shorter distance to the origin of the robotic manipulator's coordinate system was ranked higher in order to reduce the total execution time for the measurement.

The angle of the ranked leaves relative to the horizontal line were determined, which in turn was used to calculate the angle of the last joint of the robotic manipulator (the fourth joint) to have an appropriate angle for leaf grasping (Fig. 6).

The 'regionprops' function in MATLAB returns the sets of properties of connected objects in a binary image. The 'MajorAxisLength' and 'Orientation' properties in 'regionprops' function were used to calculate the length of major axis of each ranked leaf (in pixels) and to compute the angle of the ranked leaves relative to the horizontal line (in degrees).

3D plant point cloud: To visualize a 3D model of the plant, the 3D point clouds of plant was generated by creating a 3D plot of the plant pixels XYZ coordinates which were provided by the TOF camera.

2.3. Inverse kinematics of the robotic manipulator

The translation from the robotic manipulator's coordinate system to the camera's coordinate system was 10.5 cm, −4 cm, and 41.2 cm in X, Y, and Z directions (Fig. 7).

A transformation matrix was determined based on the rotation and the translation of the camera's coordinate system relative to the robotic manipulator's coordinate system (Eq. (1)).

$$^{R}P = {}^{R}_{C}T \times {}^{C}P \tag{1}$$

Where:

$${}^{R}_{C}T = \begin{bmatrix} 1 & 0 & 0 & P_x \\ 0 & \cos(90) & -\sin(90) & P_y \\ 0 & \sin(90) & \cos(90) & P_z \\ 0 & 0 & 0 & 1 \end{bmatrix}$$

^{R}P is the 3D coordinates of the center point of the leaf relative to the robotic manipulator's coordinate system; ${}^{R}_{C}T$ is the transformation matrix between the camera's coordinate system and the robotic manipulator's coordinate system; ^{C}P is the 3D coordinates of the center point of the leaf relative to the camera's coordinate system. P_x, P_y, and P_z are the translation from the robotic manipulator's coordinate system to the camera's coordinate system in X, Y, and Z directions. The transformation matrix was used to convert the 3D coordinates of the leaf's center point from the camera's coordinate system to the robotic manipulator's coordinate system (Eqs. (2)–(4)).

$$X_R = X_C + P_x \tag{2}$$

$$Y_R = -Z_C + P_y \tag{3}$$

$$Z_R = Y_C + P_z \tag{4}$$

Where:

X_C, Y_C, and Z_C are the x, y, and z coordinates of the center point of the leaf relative to the camera's coordinate system. X_R, Y_R, and Z_R are the x, y, and z coordinates of the center point of the leaf relative to the robotic manipulator's coordinate system.

The geometric approach was applied to calculate the joint angles of the robotic manipulator. Two different paths were found based on the inverse kinematics solutions. The path that gave a lower probability of hitting leaves by the robotic manipulator during grasping was chosen.

All equations for the inverse kinematics of the robotic manipulator were then derived for the chosen path. The angles of Joints 1 through 4 were calculated using Eqs. (5), (7), (6), and (8), respectively.

$$\theta_1 = atan2(X_R, Y_R) \tag{5}$$

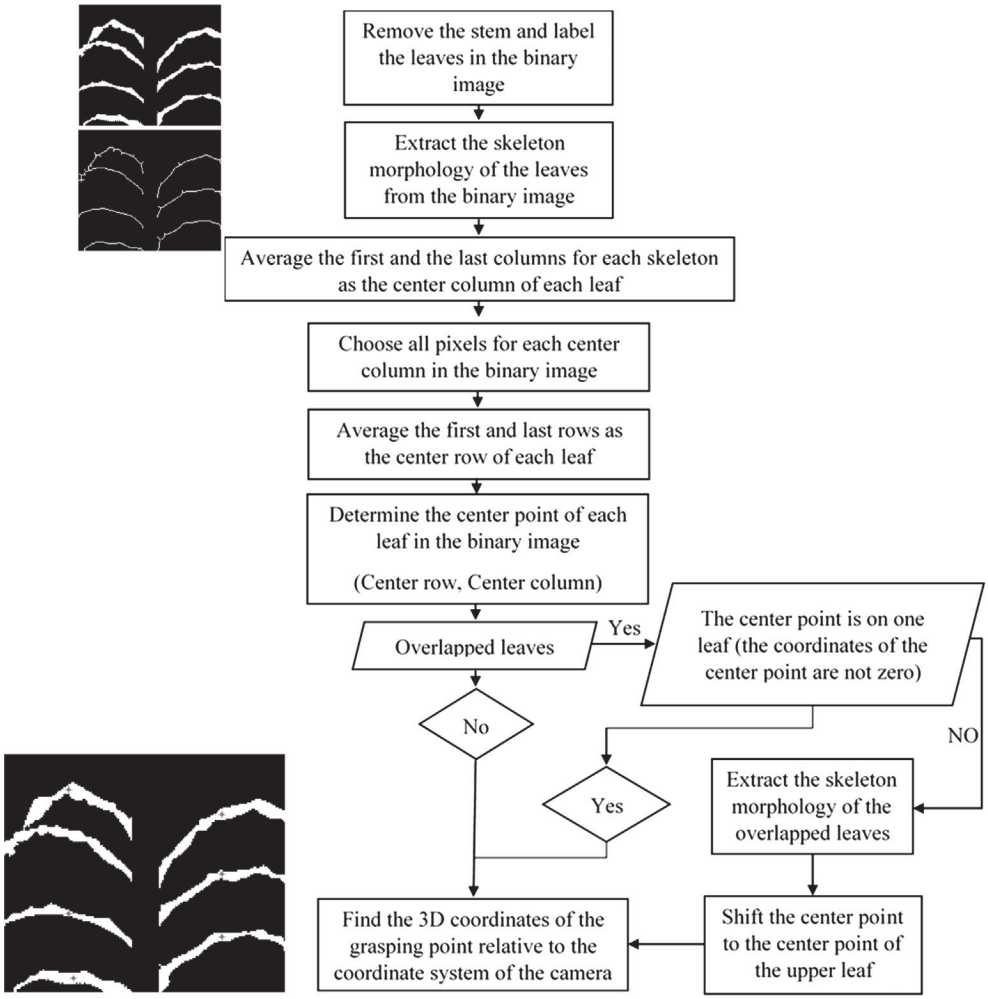

Fig. 5. Flowchart for finding the grasping point on the leaves.

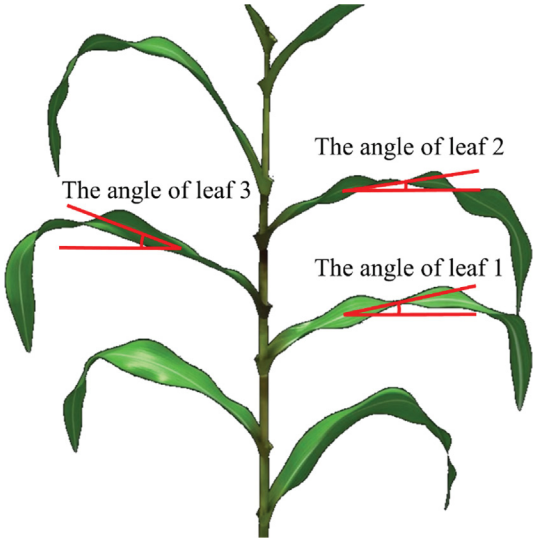

Fig. 6. Illustration of three best candidate leaves ranked and their angles relative to the horizontal line.

$$\theta_3 = atan2(\sin\theta_3, \cos\theta_3) \quad (6)$$

Where:

$$\cos\theta_3 = (X_R^2 + Y_R^2 + (Z_R - D_1)^2 - D_2^2 - L^2)/(2 \times D_2 \times L)$$

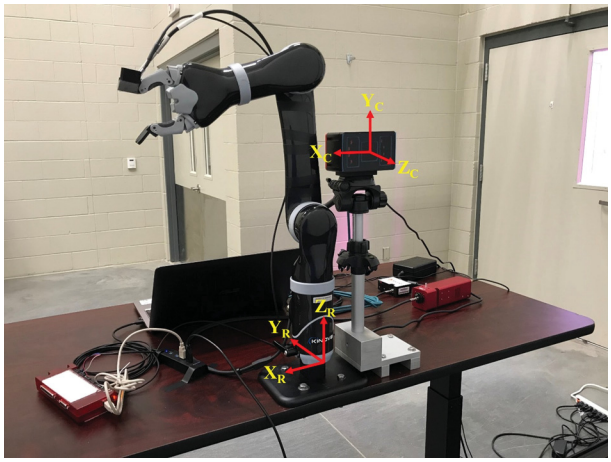

Fig. 7. Position of the coordinate system of the TOF camera ($X_CY_CZ_C$) and that of the robotic manipulator ($X_RY_RZ_R$).

$$\sin\theta_3 = \sqrt{1 - (\cos\theta_3)^2}$$

$$\theta_2 = atan2(Z_R - D_1, \sqrt{(X_R^2 + Y_R^2)}) - atan2(L \times \sin\theta_3, D_2 + L \times \cos\theta_3) \quad (7)$$

$$\theta_4 = (The\ \ angle\ \ of\ \ the\ \ leaf) + 90 \quad (8)$$

Where:

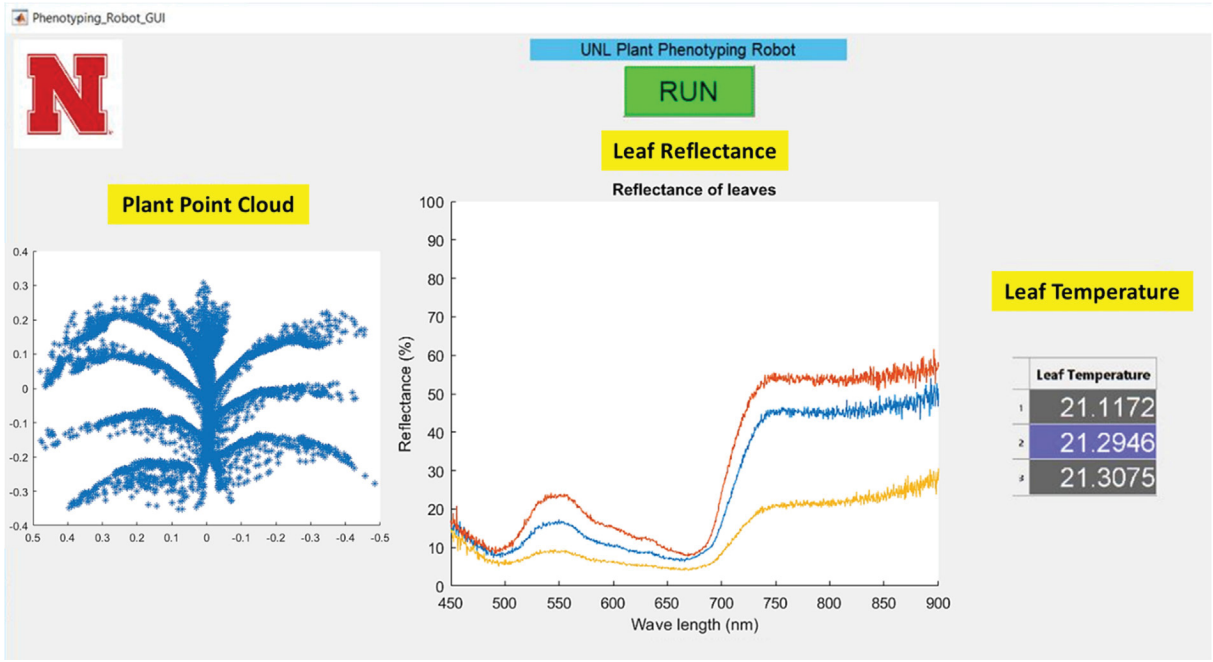

Fig. 8. The Graphic User Interface (GUI) developed in MATLAB to control the plant phenotyping robot and display the robotic measurements.

$$L = D_3 + D_4 + D_5$$

The robotic manipulator grasped the ranked leaves in two steps. First, it moved toward the leaf and then stopped at a distance ~5 cm in front of the leaf. Second, it moved horizontally to grasp the leaf. After measuring the leaf reflectance and leaf temperature, the robotic manipulator followed the same path back to the initial position.

A Graphic User Interface (GUI) was developed in MATLAB (version 2017, MathWorks, Natick, MA) to control the portable spectrometer and the thermistor and measure leaf reflectance and temperature. The GUI displayed and stored 3D point clouds of the plants (from the TOF camera), the VisNIR reflectance of the leaves, and leaf temperature readings (Fig. 8). The GUI also integrated the image processing algorithm and inverse kinematics calculation as described above. It stored the times for image processing, inverse kinematics calculation, leaf approaching and grasping, sensing process, and the total execution time (which was the time that the robotic system accomplished the entire task).

2.4. Testing and data analysis

To test the function and performance of the phenotyping robot, an experiment was conducted in the Greenhouse Innovation Center of the University of Nebraska-Lincoln. This greenhouse was equipped with a high-throughput plant phenotyping system (Scannalyzer3D, LemnaTec GmbH, Aachen, Germany). During test, the robotic system was emplaced alongside the system's conveyor belt. Plants were loaded onto the conveyor belt and transported to the system for robotic phenotyping. The distance between the camera and the plants was 20–30 cm.

Sixty maize (B73) and sixty sorghum plants (TX430) were grown in the pots and used to evaluate the robotic system. The experiment included two levels of water treatment (well-water versus water-limitation) and two levels of applied nutrients (high versus low). Each plant was randomly assigned to one of the four treatment combinations, and the goal was to create a large variation in plant leaf properties (reflectance spectra and temperature) to validate automated robotic measurements. The well-water treatment was achieved by watering pots to 80% of field capacity on a daily basis, while the water-limitation treatment 40% of field capacity. The high-nutrient treatment was achieved by adding 0.122 kg of Osmocote Plus fertilizer (15-9-12 (N-P-K) with micronutrients, 3–4 months nutrient release) into pot mix (5.67 L) at the time of planting. For low nutrient level, fertilizer liquid with 100 ppm concentration of 20-10-20 (N-P-K) fertilizer with micronutrients were added.

Data collection started when the plants were at nine leaf stage and lasted until the plants were at 13 leaf stage. The experiment was done in six weeks. Five days were chosen in each week for data collection; and in each day, data were collected from four plants with different combination of water and nutrient treatments.

Immediately after robotic phenotyping, ground-truth measurements (manual measurements by a researcher) were taken to compare with automated robotic measurements (automated measurements). A spectroradiometer (Model: FieldSpec4, Analytical Spectral Devices Inc., Longmont, CO, USA), a thermistor (Model: ST 200: Fine-Wire Thermistor, Apogee Instruments Inc., Logan, UT, USA), and a handheld chlorophyll meter (Model: MC-100 Chlorophyll Concentration Meter, Apogee Instruments Inc., Logan, UT, USA) were used to measure leaf reflectance, leaf temperature, and leaf chlorophyll content at the grasping points (Fig. 9). For each plant, up to three ground-truth and automated robotic measurements (from three grasping points identified by the robots) were made. They were averaged to represent the measurements for that plant.

After the automated and ground-truth measurement, the plant was harvested and the fresh weight of aboveground biomass was recorded. After drying the plant for 72 h at 50 °C to constant weight, leaf water content (on a fresh biomass basis) was calculated. The dried leaves of the plants were sent to a commercial lab (Midwest Laboratories, Omaha, NE, USA) and leaf Nitrogen (N), Phosphorus (P), and Potassium (K) concentrations were measured.

For the VisNIR spectra from the OceanOptics spectrometer (robotic measurements), a range from 450 to 950 nm was used (to avoid high noise regions at the two ends of spectra) for modeling and predicting leaf chemical properties. Spectra were smoothed with a moving average window (of size 30) to further reduce the noise of spectra. Similarly, spectra from the ASD spectrometer were also truncated between 450 and 950 nm for modeling and prediction. Partial least squares regression (PLSR) models of different leaf properties were calibrated using the spectra with six random segment cross-validation (60% for cross-validation and 40% for validation). Data analysis was performed in R

Fig. 9. Ground-truth measurements by a researcher: leaf reflectance spectrum (left), leaf temperature (middle), and leaf chlorophyll content (right).

Statistical Software (R Core Team, 2018) with the following packages: pls (Mevik et al., 2016), caret (Kuhn et al., 2017), and zoo (Zeileis and Grothendieck, 2005).

Two different success rates were defined and calculated for the robotic system in order to assess its performance to grasp leaves and collect data in the greenhouse.

(1) The integration success rate: It was defined as grasping at least one leaf per plant and recording the measurements successfully before releasing the plants from the robotic station.
(2) The grasping success rate: It was defined as the ratio between the number of the leaves which were successfully grasped and the total number of the leaves identified as the candidate grasping leaves.

3. Results and discussion

3.1. The performance of the robotic system

Table 1 gives summary statistics of the execution time for image processing, inverse kinematics, leaf grasping, sensing process, and total execution time to measure one leaf for maize and sorghum plants. Leaf grasping, which involved bringing the robotic gripper and sensors into contact with the leaves, took the longest time to execute. Image processing was computationally more intensive than inverse kinematics and thus took longer to execute.

The execution times for different steps and total execution time were comparable for maize and sorghum plants, and it was approximately 37 s to take one robotized measurement. This was significantly longer than human based measurement, which only took 5–6 s in our case.

Table 1
Summary statistics for the execution time of different steps in automated robotic measurement of one leaf.

Time (s)	Statistic	Maize plant	Sorghum plant
Image processing	Maximum	3.86	4.30
	Minimum	2.32	1.89
	Average	3.05	2.64
	Standard deviation	0.412	0.470
Inverse kinematics	Maximum	0.049	0.060
	Minimum	0.016	0.013
	Average	0.026	0.026
	Standard deviation	0.009	0.009
Leaf grasping	Maximum	45.5	45.1
	Minimum	22.5	22.2
	Average	31.5	33.6
	Standard deviation	5.17	5.79
Sensing process	Maximum	2.44	1.75
	Minimum	0.845	0.858
	Average	1.19	1.24
	Standard deviation	0.356	0.344
Total execution	Maximum	47.2	52.9
	Minimum	30.3	29.2
	Average	35.5	38.5
	Standard deviation	4.39	5.68

The image processing to segment the leaves from the stem worked well for maize plants. However, the specific variety of sorghum we chose to work with (TX430) exhibited more vertically distributed leaves than maize. This sorghum morphology made it more challenging to remove stem pixels while retaining leaf pixels for leaf identification and grasping point localization (Figs. 4 and 5). For this reason, the integration success rate was only 48% for sorghum plants, much lower than 78% for maize plants.

The grasping success rate for maize plants was 50% and that for sorghum plants was similar (~50%). The experiment also showed that the phenotyping robot could grasp on average two leaves per plant and collect data successfully. It failed to grasp a leaf for three main reasons. First, if the 3D coordinates of the grasping point were out of the workspace of the robotic manipulator, the robotic manipulator was not driven to grasp the leaf. Second, since the camera had uncertainty to measure the z coordinate of the scene (± 2 cm), it could cause an error in the calculation of the joint angles of the robotic manipulator and only grasped the target leaf partially at the edge of the leaf. Third, if the leaf was vertical (i.e. approximately 90° angle from the horizontal plane), the manipulator could not grasp the leaf due to the lack of needed dexterity and degree of freedom.

Fig. 10 compares the leaf temperature of maize and sorghum plants measured by the human operator (ground-truth) with that measured by the phenotyping robot. It can be seen that two sets were significantly linearly correlated (R^2 = 0.58 for maize plants, R^2 = 0.63 for sorghum, and R^2 = 0.62 for maize and sorghum plants together). However, there was also significant bias between them. Robotized temperature measurement was 0.71 °C lower than the manual measurement in maize, 0.81 °C lower in sorghum, and 0.76 °C in both species together. Three factors could be attributed to the bias between the two temperature measurements. Firstly, when the human operator took the temperature measurement, she always ensured good contacts between the leaf and the sensor. This was quite challenging for our phenotyping robot, which

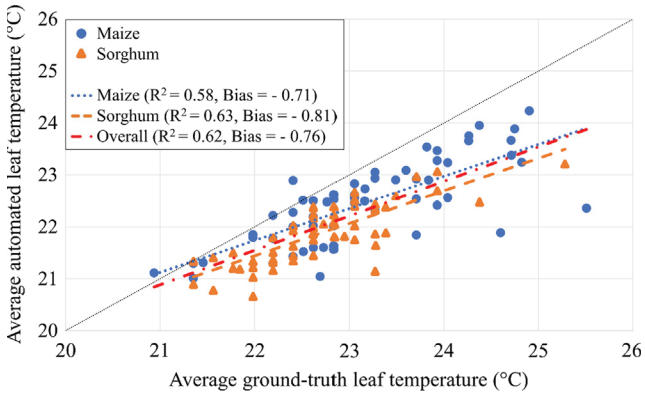

Fig. 10. Scatterplot of leaf temperature measured by the human operator versus the phenotyping robot for maize and sorghum plants. The linear regression and the statistics were reported for maize, sorghum, and the two species together.

lacked the needed dexterity, degree of freedom, and the sense of pressure to orient its manipulator and gripper nicely with the leaf surface to have a good contact. This could explain the negative bias of the robotized measurements. The second factor could be due to the fast change of leaf temperature relative to ambient temperature. There were large temperature differences between the greenhouse (where the plants were grown) and the head house (where the measurements were taken). Leaf temperature was likely not in a steady state during measurement. There was a slight time difference between the manual and robotic measurement, which would lead to small bias between the two sets of temperature measurements. Thirdly, the two temperature sensors used by the human operator and the phenotyping robot were not cross calibrated. They could indicate a temperature different as large as 0.5 °C even when they were to measure the same object; and the sensor used by the human operator were known to indicate slightly higher temperature.

We further conducted a Welsh's two-sample *t*-test to compare leaf temperature of the plants under the two water treatments. The rationale for this comparison was that the plants under the water limitation treatment should exhibit higher leaf temperature due to the drought effect of reduced leaf-level transpiration (Fig. 11). The results showed that, for maize plants, leaf temperature was significantly higher (p-value = 0.018) when measured manually by the human operator. However, such difference was not significant (p-value = 0.111) for the automated robotic measurements, even though the mean temperature for the water limitation group was slightly higher. For sorghum, neither manual measurements nor robotic measurements exhibited significant difference between the two water treatment groups (p-values = 0.245 and 0.068, respectively). Sorghum is more drought tolerant than maize, which could explain the non-significant leaf temperature difference. Although there is still improvement to make robotized leaf temperature measurements more accurate, this comparison suggested one potential use of our phenotyping robot to distinguish drought-tolerant lines from drought-sensitive lines.

3.2. Chemometric prediction of leaf chemical properties from leaf reflectance data

Table 2 gives results of PLSR modeling of leaf chemical properties using leaf reflectance spectra measured by the phenotyping robot in comparison to manual measurements. Among the five leaf properties studied, leaf chlorophyll content was predicted most successfully, followed by fresh-based water content and K. Prediction of N and P exhibited poorer performance. Fig. 12 shows the scatterplots of predicted versus measured leaf properties in maize and sorghum for both manual and robotic measurements.

The predictions with spectra data from the ASD spectrometer were substantially better than with those from the OceanOptics spectrometer. Note that ASD spectra were acquired with a human operator, whereas OceanOptics spectra were acquire automatically with the phenotyping robot. During spectral data collection, the human operator always ensured that the leaf clip was in close contact with the leaf. In many occasions, she was using the other hand to guide the orientation of the leaf blade such that no light was leaked out of the measurement point. This kind of manipulation was very difficult to achieve with our phenotyping robot, again due to the lack of needed dexterity and the sense of pressure to ensure good contacts between the gripper and the leaf. This resulted light leakage and thus lower spectral quality in leaf reflectance measurement.

3.3. Potential improvements and future directions

We developed and demonstrated a robotic system that can realize *in vivo*, human-like measurements of plant leaf traits in the greenhouse. This approach was different from the traditional image-based phenotyping, where plant images were used as a nondestructive means to acquire predominantly morphological traits such as height, width and projected leaf area (Neilson et al., 2015; Ge et al., 2016). Even though some imaging modules such as NIR and hyperspectral imaging can probe leaf biochemical traits (Pandey et al., 2017), they still need manual measurements to establish correlations with image data. In this sense, the phenotyping robot would be useful to complement image-based phenotyping by obtaining physiological or chemical measurements directly at the plant leaf level.

We integrated to the robotic gripper a fiber optical cable to measure leaf-level reflectance and a thermistor to measure leaf temperature. With some mechanical modifications, sensors to measure other leaf properties (such as stomatal conductance, gas exchange, chlorophyll content, etc.) can be integrated. It is also possible to integrate a mechanical sampler to cut and collect leaf disks with the robotic gripper. While the measurement speed of the phenotyping robot is slower than that of a human operator, many of these robots (equipped with different plant sensors) can be launched in the greenhouse, which would substantially enhance the speed and capacity of the phenotyping robot. Furthermore, many modern greenhouses already have conveyor systems to move the plants around, which would make the integration of the phenotyping robots with the existing greenhouse infrastructure straightforward.

The phenotyping robot realized its designed functions of automated leaf probing and leaf-level trait measurement. Its performance, nevertheless, could be further improved. Firstly, a robotic manipulator with more DOF would make the robot more dexterous and flexible to probe the leaves. This measure would ensure good contact between the gripper/sensors and plant leaves, which is critical to improve the quality of sensor measurements. Secondly, a collision free path planning algorithm would be designed and implemented. This technique finds the optimal path for the robotic manipulator's movements between two grasping points without hitting the leaves or stem and potentially reduces execution time. Thirdly, the TOF camera we used is low in spatial resolution and introduces large uncertainties in

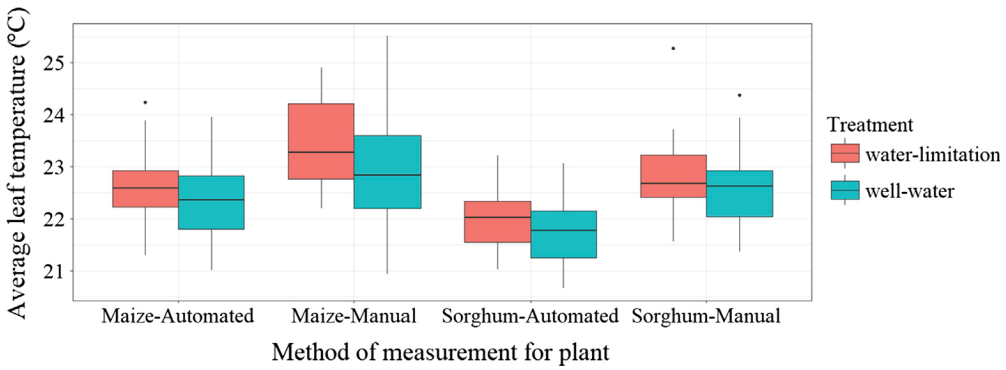

Fig. 11. The box plots of average manual vs. automated leaf temperatures for maize and sorghum plants with two water treatments.

Table 2
Results of partial least squares modeling to predict leaf chemical properties using leaf reflectance spectra measured by the phenotyping robot in comparison to manual measurements.

Property	Manual						Robotic					
	Cross-validation			Validation			Cross-validation			Validation		
	R^2	RMSE	Bias	R^2	RMSE	Bias	R^2	RMSE	Bias	R^2	RMSE	Bias
CHL (μmol/m^2)	0.907	57.9	0	0.865	69.0	−11.0	0.664	119	0	0.525	112	−1.12
FBWC (%)	0.891	1.97	0	0.861	2.25	0.517	0.637	3.46	0	0.614	3.75	1.12
N (%)	0.602	0.271	0	0.384	0.333	−0.078	0.421	0.331	0	0.139	0.374	−0.036
P (%)	0.567	0.112	0	0.565	0.114	−0.003	0.406	0.139	0	0.112	0.230	−0.063
K (%)	0.870	0.500	0	0.788	0.667	−0.027	0.693	0.835	0	0.519	1.00	0.020

CHL = Chlorophyll content, FBWC = Fresh-based water content, N = Nitrogen, P = Phosphorus, K = Potassium, RMSE = Root mean squared error.

determining the XYZ coordinates of grasp points. Using a stereovision camera with higher accuracy can improve grasp point localization, and therefore improve the overall success rate of leaf probing and robotic measurements. Finally, the test plants were all placed with their symmetrical plane facing the TOF camera. In this position, leaf occlusion was minimized which was instrumental to subsequent image processing and robotic measurements. In real applications, plants would be randomly oriented and presented to the imaging system, therefore causing a number of problems regarding leaf segmentation and robotic measurements. These challenges need to be sufficiently tested and

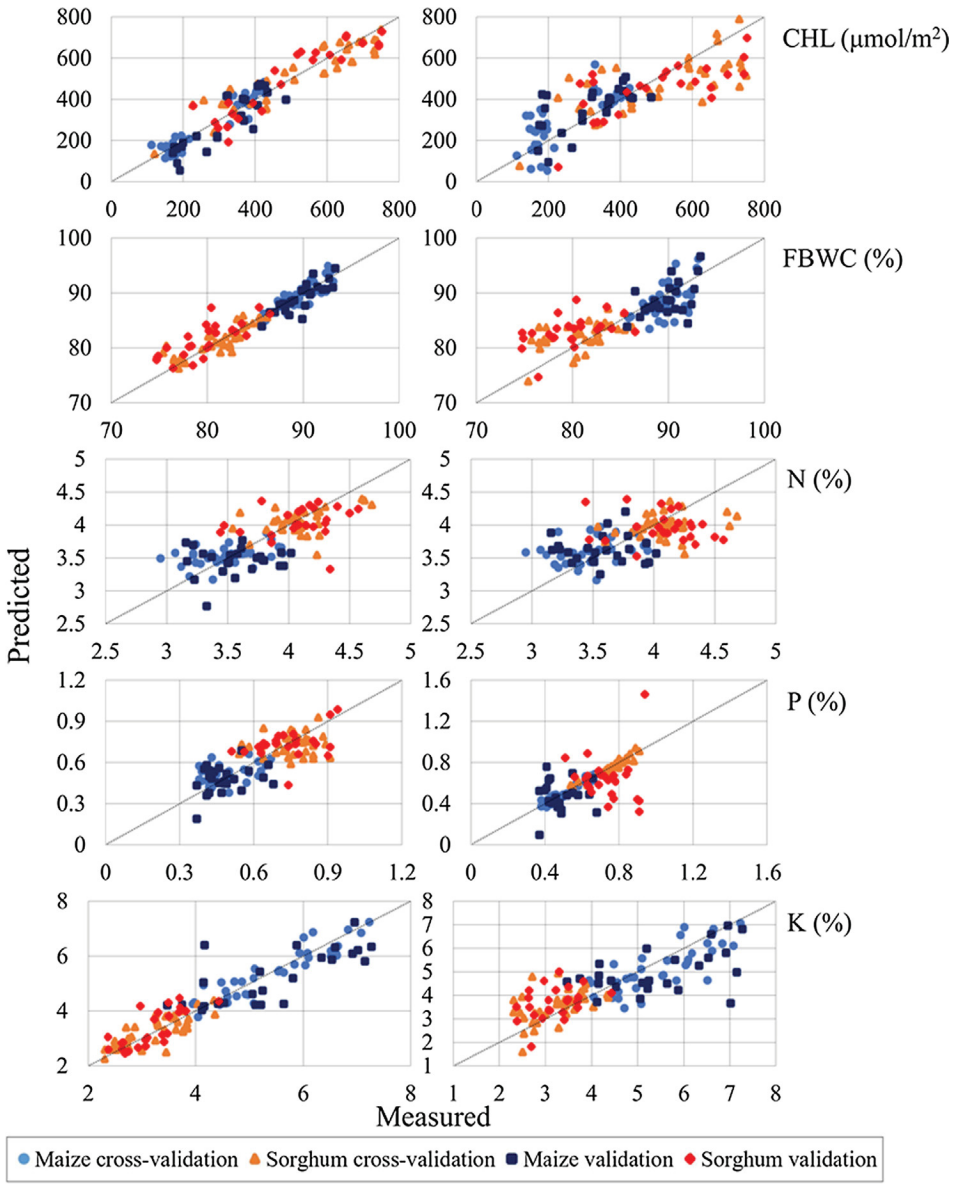

Fig. 12. Scatterplots of lab-measured versus predicted leaf properties of maize and sorghum plants for manual measurement (left column) and robotic measurement (right column).

addressed for real life applications.

4. Conclusions

In this paper, we designed and developed a plant phenotyping robotic system to realize *in vivo*, human-like leaf trait measurement. The system comprised of a 3D TOF camera, a four DOF robotic manipulator, and a custom-made gripper that integrated a bifurcated fiber optic cable and a thermistor. This robotic system was tested in the greenhouse using maize and sorghum plants. The test result showed moderate accuracy for measuring several leaf traits including temperature, chlorophyll content, fresh-based water content, and potassium (R^2 ranged from 0.52 to 0.62) by the phenotyping robot in comparison to the ground-truth measurement. The leaf grasping success rate was ~50% for both maize and sorghum, and the average execution time to take measurements from one leaf was 35.5 s for maize and 38.5 s for sorghum. This phenotyping robot has the great potential to complement image-based high-throughput plant phenotyping by measuring leaf physiological and chemical traits directly and automatically.

Acknowledgment

This work was supported by USDA-NIFA, United States (Award# 2017-67007-25941). The authors would like to thank Greenhouse staff Vincent Stoerger and Troy Pabst for their assistance in experiment design and plant caring, and undergraduate student Ema Muslic for her assistance in data collection.

References

Ahlin, K., Joffe, B., Hu, A.-P., McMurray, G., Sadegh, N., 2016. Autonomous leaf picking using deep learning and visual-servoing. IFAC-PapersOnLine 49, 177–183. https://doi.org/10.1016/j.ifacol.2016.10.033.

Alenyà Ribas, G., Dellen, B., Foix Salmerón, S., Torras, C., 2012. Robotic leaf probing via segmentation of range data into surface patches. In: Proceedings of the 2012 IROS Workshop on Agricultural Robotics: Enabling Safe, Efficient, Affordable Robots for Food Production. pp. 1–6.

Andrade-Sanchez, P., Gore, M.A., Heun, J.T., Thorp, K.R., Carmo-Silva, A.E., French, A.N., Salvucci, M.E., White, J.W., 2014. Development and evaluation of a field-based high-throughput phenotyping platform. Funct. Plant Biol. 41, 68–79.

Bai, G., Ge, Y., Hussain, W., Baenziger, P.S., Graef, G., 2016. A multi-sensor system for high throughput field phenotyping in soybean and wheat breeding. Comput. Electron. Agric. 128, 181–192.

Bai, G., Ge, Y., Scoby, D., Leavitt, B., Stoerger, V., Kirchgessner, N., Irmak, S., Graef, G., Schnable, J., Awada, T., 2019. NU-Spidercam: a large-scale, cable-driven, integrated sensing and robotic system for advanced phenotyping, remote sensing, and agronomic research. Comput. Electron. Agric. 160, 71–81.

Bao, Y., Tang, L., Shah, D., 2017. Robotic 3D plant perception and leaf probing with collision-free motion planning for automated indoor plant phenotyping. In: 2017 ASABE Annu. Int. Meet., ASABE Paper No. 1700369. https://doi.org/10.13031/aim.201700369.

Chaudhury, A., Ward, C., Talasaz, A., Ivanov, A.G., Brophy, M., Grodzinski, B., Huner, N., Patel, R. V, Barron, J.L., 2017. Machine Vision System for 3D Plant Phenotyping. arXiv Prepr. arXiv1705.00540.

Fischer, G., 2009. World food and agriculture to 2030/50. In: Technical Paper from the Expert Meeting on How to Feed the World In. pp. 24–26.

Foix, S., Alenyà, G., Torras, C., 2015. 3D Sensor planning framework for leaf probing. In: 2015 IEEE/RSJ International Conference on Intelligent Robots and Systems (IROS). pp. 6501–6506. https://doi.org/10.1109/IROS.2015.7354306.

Fourcaud, T., Zhang, X., Stokes, A., Lambers, H., Körner, C., 2008. Plant growth modelling and applications: the increasing importance of plant architecture in growth models. Ann. Bot. 101, 1053–1063.

Ge, Y., Bai, G., Stoerger, V., Schnable, J.C., 2016. Temporal dynamics of maize plant growth, water use, and leaf water content using automated high throughput RGB and hyperspectral imaging. Comput. Electron. Agric. 127, 625–632.

Kirchgessner, N., Liebisch, F., Yu, K., Pfeifer, J., Friedli, M., Hund, A., Walter, A., 2017. The ETH field phenotyping platform FIP: a cable-suspended multi-sensor system. Funct. Plant Biol. 44, 154–168.

Klose, R., Möller, K., Vielstädte, C., Ruckelshausen, A., 2010. Modular system architecture for individual plant phentotyping with an autonomous field robot. In: Proceedings of the 2nd International Conference of Machine Control & Guidance, pp. 299–307.

Kuhn, M., Wing, J., Weston, S., Williams, A., Keefer, C., Engelhardt, A., Cooper, T., Mayer, Z., Kenkel, B., Team, the R.C., Benesty, M., Lescarbeau, R., Ziem, A., Scrucca, L., Tang, Y., Candan, C., Hunt., T., 2017. caret: Classification and Regression Training.

Neilson, E.H., Edwards, A.M., Blomstedt, C.K., Berger, B., Moller, B.L., Gleadow, R.M., 2015. Utilization of a high-throughput shoot imaging system to examine the dynamic phenotypic responses of a C4 cereal crop plant to nitrogen and water deficiency over time. J. Exp. Bot. 66, 1817–1832.

Lu, H., Tang, L., Whitham, A.S., Mei, Y., 2017. A robotic platform for corn seedling morphological traits characterization. Sensors. https://doi.org/10.3390/s17092082.

Mevik, B.-H., Wehrens, R., Liland, K.H., 2016. pls: Partial Least Squares and Principal Component Regression.

Mueller-Sim, T., Jenkins, M., Abel, J., Kantor, G., 2017. The Robotanist: A ground-based agricultural robot for high-throughput crop phenotyping. In: 2017 IEEE International Conference on Robotics and Automation (ICRA), pp. 3634–3639. https://doi.org/10.1109/ICRA.2017.7989418.

Pandey, P., Ge, Y., Stoerger, V., Schnable, J.C., 2017. High throughput in vivo analysis of plant leaf chemical properties using hyperspectral imaging. Front. Plant Sci. 8, 1348.

R Core Team, 2018. R: A language and environment for statistical computing. R Foundation for Statistical Computing, Vienna, Austria. URL https://www.R-project.org/.

Rahaman, M.M., Chen, D., Gillani, Z., Klukas, C., Chen, M., 2015. Advanced phenotyping and phenotype data analysis for the study of plant growth and development. Front. Plant Sci. 6, 619.

Shafiekhani, A., Kadam, S., Fritschi, B.F., DeSouza, N.G., 2017. Vinobot and vinoculer: two robotic platforms for high-throughput field phenotyping. Sensors. https://doi.org/10.3390/s17010214.

Shah, D., Tang, L., Gai, J., Putta-Venkata, R., 2016. Development of a mobile robotic phenotyping system for growth chamber-based studies of genotype x environment interactions. IFAC-PapersOnLine 49, 248–253. https://doi.org/10.1016/j.ifacol.2016.10.046.

Van Henten, E.J., Van Tuijl, B.A.J., Hoogakker, G.-J., Van Der Weerd, M.J., Hemming, J., Kornet, J.G., Bontsema, J., 2006. An autonomous robot for de-leafing cucumber plants grown in a high-wire cultivation system. Biosyst. Eng. 94, 317–323. https://doi.org/10.1016/j.biosystemseng.2006.03.005.

Vijayarangan, S., Sodhi, P., Kini, P., Bourne, J., Du, S., Sun, H., Poczos, B., Apostolopoulos, D., Wettergreen, D., 2018. High-Throughput Robotic Phenotyping of Energy Sorghum Crops. In: Hutter, M., Siegwart, R. (Eds.), Field and Service Robotics. Springer International Publishing, Cham, pp. 99–113.

Virlet, N., Sabermanesh, K., Sadeghi-Tehran, P., Hawkesford, M.J., 2017. Field Scanalyzer: an automated robotic field phenotyping platform for detailed crop monitoring. Funct. Plant Biol. 44, 143–153.

Xiao, D., Gong, L., Liu, C., Huang, Y., 2016. Phenotype-based robotic screening platform for leafy plant breeding. IFAC-PapersOnLine 49, 237–241. https://doi.org/10.1016/j.ifacol.2016.10.044.

Yendrek, C.R., Tomaz, T., Montes, C.M., Cao, Y., Morse, A.M., Brown, P.J., McIntyre, L.M., Leakey, A.D.B., Ainsworth, E.A., 2017. High-throughput phenotyping of maize leaf physiological and biochemical traits using hyperspectral reflectance. Plant Physiol. 173, 614–626.

Zeileis, A., Grothendieck, G., 2005. zoo: S3 infrastructure for regular and irregular time series. J. Stat. Softw. 14, 1–27. https://doi.org/10.18637/jss.v014.i06.